

P6.1

THE DOPPLER WEATHER RADAR NOWCASTING TOOL GSF, APPLICATION AT THE EUROPEAN SPACEPORT FOR THE SUPPORT OF ARIANE 4 / 5 ROCKET LAUNCHES

Matthias Toussaint*, , Martin Malkomes*, GAMIC, Germany
Isabelle Donet**, Arnaud Carlier**, CSG, ,French Guyana

1. INTRODUCTION

The Nowcasting tool (GSF) installed at the French Guyana Space Center, Europe's spaceport (CSG).is presented The C-Band Doppler weather radar system ROMUALD "Radar d'Observation Météo d'Utilisation Aisée Localement et à Distance" is used as the sensor for generation of input data for the tracking and forecasting (Nowcasting) process.

The GSF software is designed to automatically assist to the real time weather watch and automatic forecast at operational meteorological services. At CSG the GSF is integrated into the multi-user networked meteorological software environment FROG (Fast Radar Observation by GAMIC) designed for real-time weather analysis.

This system yields an effective tool to forecast high risk and risk area due to meteorological phenomena (Weather systems causing electrical discharges, severe winds) in the operational rocket launch pad environment at CSG.

The installation and adaptation of the GSF system resulted from close cooperation between the CSG operational users, the Centre National d'Etudes Spatiales CNES, and the contracted company GAMIC each having contributed the specific software and operational meteorological know how.

2. OPERATIONAL REQUIREMENTS

The following topics are of vital importance for operationally working meteorologists:

2.1 Calculation of echo displacement

The first part of GSF is an extension of the tracking algorithm developed in 1995 by GAMIC [M. Unger, COST 73]. Cross-correlation methods with additional application of continuity constraints yield good results: The second GSF part is based on the cross-correlation method, TREC [Rinehart, 1978] and COTREC [Li, 1995] with extensions as published [A. Zgonc, COST 75].

By use of similarity criteria a set of displacement vectors is derived for image cells and clusters.

2.2 Cell and cloud system forecast calculation

The forecast is calculated by means of the calculation of the motion vector field of echo patterns. By this motion vector field each cell has an individual forecast vector which may differ from the

Corresponding author addresses: **CNES-CSG, CG/SDO/ME/LC/MT, Kourou 97310, French Guyana, e-mail: Isabelle.Donet@cnes.fr

*GAMIC mbH, 52072 Aachen, Roermonder Str. 151, Germany, e-mail: malkomes@gamic.com

the neighbour cells. Non uniform cell movements are as well detected and used for the cell forecast. The forecast of the future cell position is derived from the forecast vector related to each cell. Linear time extrapolation is performed by using growth and decay models. Continuity in time and angular direction is assumed.

2.3 Forecast time definition

Reliable predictions can be made for 1-2 h in stratiform cases, 20-40 min for convective air masses. A forecast quality factor (%) is derived which continuously checks the "old" forecast against the current real product.

2.4 Preceding image use

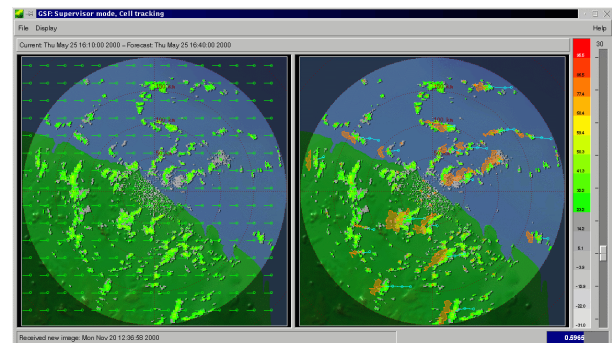
The number of images used is limited by the radar range and the mean displacement time of the air mass. The algorithm is not restricted to the number of images but to the validity of continuity assumption the growth/decay of cells in the convective case.

3. THEORY OF OPERATION

The GSF forecasting algorithm based on products like PPI(Z,R), CAPPI(Z,R) or MAXCAPPI(Z,R). Two independent forecasting algorithms are available:

- Cloud cell tracking [Paper Cost 75, M. Unger]
- TREK motion field tracking [Paper Cost 75, Anton Zgonc, Prof. Joze Rakovec]

Both algorithms have different performance depending on the weather situation.



3.1 Cloud cell tracking

This algorithm gives best results with small cloud cells found in the radar range for three or more scans. The following steps are performed within the tracking algorithm.

• Threshold check

This is used for identification of a cell or area that reach minimum specified precipitation over an area.

Area with little or no precipitation will be disregarded.

- **Segmentation**

The radar range is separated into segments. Only segments having coverage larger than a_{min} are considered.

- **Segment matching**

All thresholded segments are compared to their neighboring segments of the previous radar image. Only segments with a maximum distance less than r_{max} are compared. The value of r_{max} is calculated via the user defined maximum expected wind speed. The cells with a correlation coefficient greater than c_{min} are taken into. The threshold value c_{min} is user defined.

- **Filtering**

The mean "product" displacement vector is calculated. All segment displacement with an angle differing more than a_{max} from the mean displacement vector are discarded

- **Generation of forecast image**

The forecast image is generated by translation of the segments with their displacement vector extrapolated to the forecast time. The remaining segments (without individual translation vector) are translated via the average of all vectors found.

3.2 TREC/COTREC

This algorithm is an implementation of the TREC algorithm (Rinehart and Garvey, 1978) and its derivation COTREC (Li et al., 1995). The algorithm computes a motion vector field over the entire scan area. Based on this motion vector field the forecast image is time extrapolated.

- **Threshold check**

To identify cells with minimum precipitation

- **Segmentation**

The current radar image is divided into rectangular cells with a user defined size. The cell size should be large enough to embody typical shapes of radar echoes (i.e. about $10 \times 10 \text{ km}^2$ or larger)

- **Computation of mean displacement vector for performance improvement**

Now a mean displacement vector \mathbf{a} for the complete radar image is calculated via correlation with the previous image. The displacement with minimum mean absolute difference is chosen. It's correlation coefficient must be greater than the user defined value c_{min} .

This step is needed for performance improvements in the next step.

In order to avoid unnecessary numerical procedures the search area in the next step is limited by the following conditions:

- Displacement radius
- Angle θ of displacement vector does not differ more than a_{max} from the mean displacement vector
- Cell contains at least e_{min} % of echoes

If the correlation coefficient is above the user definable threshold c_{min} the vector \mathbf{a} is taken for the

above mentioned limitations of the search area. Otherwise the search area is only limited by $|r|$.

- **Computation of cell displacement vectors**

Now the displacement vector is calculated for each cell using the same algorithm as for the mean displacement vector. Each cell is correlated to the previous radar image to compute the individual displacement vector. The above mentioned limitations are applied in this step. Only cells with a user definable minimum of radar echo are used for computation.

- **Filling of non echo areas**

The cells without movement vector are filled with the average vector of the calculated cells. To smooth the vector field the COTREC (Continuity of TREC vectors) [Li et al. 1995] algorithm is used. The main idea is to adjust the motion vector field so that continuity equation is fulfilled but as much of resemblance to the original field as possible is retained. For that purpose the cost function is minimized. A variational procedure yields the Poisson equation for Lagrange multiplied with boundary condition which can be numerically solved e.g. by the SOR algorithm (see e.g. Press et al., 1992). The COTREC velocity field is then obtained by smoothed vector field with filled empty cells

- **Generation of forecast image**

The local vector field is evaluated via bilinear interpolation. For each grid element separate coefficients using all four corner values are used. A Lagrangian backward-time scheme is used for determination of motion of echo patterns. The final point of each trajectory s is one of the radar grid-points r_{ij} . It is simply backward integrated to the starting point.

4. References

Li, L., Schmidt, W., and Joss, J. (1995). Nowcasting of motion and growth of precipitation with radar over a complex orography. *Journal of Applied Meteorology*, **34**, 1286-1300.

Press, W. Et. Al. (1992). *Numerical Recipes in C: the Art of Scientific Computing*. Cambridge University Press, 2nd edition.

Unger, M. (1994). Rainbow shearwind detection and warning modules for TDWR applications with Meteor 360C radar. *COST 75 Weather Radar Systems 1994*, 472-479

Rinehart, R. E. (1981). A pattern recognition technique for use with conventional weather radar to determine internal storm motions. *Atmospheric Technology*, pages 119-134

Rinehart, R. E. And Garvey, E. T. (1978). Three-dimensional storm motion detection by conventional weather radar. *Nature*, **273**, 287-189

Zgonc, A., Radovec, J. (1998). Time extrapolation of Radar Echo Patterns. *COST 75 Weather Radar Systems 1998*, 229-238